Journal of Power Sources 196 (2011) 1141–1144

Contents lists available at ScienceDirect

Journal of Power Sources

journal homepage: www.elsevier.com/locate/jpowsour

Short communication

Studies on the electrochemical reduction of oxygen catalyzed by reduced graphene sheets in neutral media

Jiajia Wu[a,b], Yi Wang[a], Dun Zhang[a,*], Baorong Hou[a]

[a] Key Lab of Corrosion Science, Shandong Province, Institute of Oceanology, Chinese Academy of Sciences, Qingdao 266071, China
[b] Graduate School of the Chinese Academy of Sciences, Beijing 100039, China

ARTICLE INFO

Article history:
Received 28 June 2010
Received in revised form 27 July 2010
Accepted 27 July 2010
Available online 6 August 2010

Keywords:
Oxygen reduction reaction
Reduced graphene sheets
Microbial fuel cell
Catalysis
Disproportionation

ABSTRACT

Reduced graphene sheets (RGSs) were prepared via chemical reduction of graphite oxide and their morphology was characterized by atomic force microscopy. The electrochemical reduction of oxygen (O_2) with RGSs was studied by cyclic, rotating disk electrode, and rotating ring-disk electrode voltammetry using the RGSs-modified glassy carbon (RGSs/GC) electrode in 3.5% NaCl solution. The results show that O_2 reduction undergoes three steps at the RGSs/GC electrode: electrochemical reduction of O_2 to H_2O_2 mediated by quinone-like groups on the RGSs surface, a direct 2-electron reduction of O_2, and reduction of the H_2O_2 produced to H_2O. The modification of RGSs results in an obvious positive shift of the peak potential and a larger current density. The kinetics study shows that the number of electrons transferred for O_2 reduction can reach to 3.0 at potentials of the first reduction step, indicating RGSs can effectively catalyze the disproportionation of H_2O_2. Such catalytic activity of RGSs enables a 4-electron reduction of O_2 at a relatively low overpotential in neutral media. RGSs are a potential electrode material for microbial fuel cells.

1. Introduction

Microbial fuel cells (MFCs) are bioreactors that generate electricity directly from the degradation of organic substances with the aid of bacteria [1–4]. Like other low-temperature fuel cells, the slow kinetics of the oxygen reduction reaction (ORR) at the cathode has limited the energy production of MFCs [5–11]. In order to improve the cathode performance, one common research interest in MFCs is the development of catalysts [12]. Platinum (Pt) is the most commonly used catalyst for the ORR in MFCs, but it suffers price, scarcity, and possible poisoning by components of the substrate or by-products [13]. Some promising non-Pt electrocatalysts have been developed, such as transition metal porphyrin and phthalocyanine [14–17], polypyrrole [18], manganese oxide [19–21], and lead dioxide [22]. Besides catalysts, the performance can also be improved by utilizing high surface area carbon materials, such as granular graphite and activated carbon fiber felt [23,24].

Graphene, discovered by Geim group in 2004 [25], is a two-dimensional flat material consisting of monolayer carbon atoms. This material exhibits excellent physical and chemical properties, such as high electrical conductivity [26,27], high surface area [28,29], and a large amount of edge-planes/defects [30], which makes it promising for potential applications in electrochemical field. There have been some studies on the catalysis of graphene and graphene-based composites for the ORR in alkaline and acid media [31–34], but few in neutral media except that Shan et al. proved its better catalytic properties than graphite with cyclic voltammetry [35]. Therefore, it is quite necessary to study systematically the catalytic activity of this material towards the ORR in neutral media for its potential application in MFCs.

In this work, we attempted to study the mechanism of the ORR at the reduced graphene sheets (RGSs) modified glassy carbon (RGSs/GC) electrode. The electrolyte used was 3.5% NaCl solution for the simple simulation of operation condition of benthic MFCs. For the first time, RGSs were found to possess an excellent catalytic activity for the 4-electron ORR with a low overpotential in neutral media.

2. Experimental

2.1. Chemicals and materials

All reagents except natural graphite powder were of analytical grade and purchased from Sinopharm Chemical Reagent Co. Ltd. (Shanghai, China). Natural graphite powder (99.99%) was supplied by Beijing Chemical Company (Beijing, China). Milli-Q water (Millipore, Bedford, MA, USA) was used in all the process of aqueous solution preparations and washings. Ultra-high purity nitrogen

* Corresponding author. Tel.: +86 532 82898960; fax: +86 532 82898960.
E-mail address: Zhangdun@qdio.ac.cn (D. Zhang).

0378-7753/$ – see front matter © 2010 Elsevier B.V. All rights reserved.
doi:10.1016/j.jpowsour.2010.07.087

(N_2) and oxygen (O_2) (Qingdao Heli Gas Co. Ltd., Qingdao, China) gases were used for the deaeration of solutions and the preparation of O_2-saturated solutions, respectively.

2.2. Synthesis and characterization of RGSs

RGSs investigated in this work were synthesized following the procedure reported by Stankovich et al. [36], which consists of three steps: preparation of graphite oxide (GO) from natural graphite according to Hummers method [37], exfoliation of GO by sonication and reduction of exfoliated GO with hydrazine hydrate.

Atomic force microscopy (AFM) image of the synthesized RGSs was taken with Nanoscope IIIa (Digital Instruments, USA) in tapping mode. After sonicating for 5 min with an ultrasonic bath cleaner, a droplet of the RGSs suspension (0.01 g L^{-1}) was cast onto freshly cleaved mica. The sample was kept at room temperature overnight to let the water evaporate.

2.3. Preparation of the RGSs/GC electrode

A rotating ring-disk electrode (RRDE, Pine Research Instrument Inc., Grove City, PA, USA) with a GC disk (5.61 mm diameter) and a Pt ring (7.92 mm outer diameter and 6.25 mm inner diameter) was used in this study. The disk electrode was polished with 1.0 and 0.05 μm alumina slurries, and then was cleaned by sonication in water for 15 min. Prior to the surface modification, as-synthesized RGSs were dispersed by sonication to form a homogenous suspension. The RGSs/GC electrode was prepared by casting the RGSs suspension on the disk electrode surface and drying in N_2 atmosphere at ambient temperature. The loading of the RGSs on the surface of GC electrode was ca. 0.2 mg cm^{-2}.

2.4. Electrochemical measurements

Cyclic, rotating disk electrode (RDE), and RRDE voltammetric electrochemical measurements were performed on a computer-controlled electrochemical analyzer (CHI 760C, CH Instruments Inc., Austin, TX, USA) with a three-electrode electrochemical cell. The bare GC and RGSs/GC electrodes were used as the working electrodes. A Pt wire and a KCl-saturated Ag/AgCl electrode were used as the counter electrode and reference electrode, respectively. The electrolyte, 3.5% NaCl solution, was bubbled with N_2 or O_2 for more than 20 min to make a solution saturated with N_2 or O_2, respectively, and a continuous flow of gases was maintained over the solutions during the electrochemical measurements. All potentials are reported versus the Ag/AgCl (KCl-sat.) electrode. RDE and RRDE measurements were conducted with a rotation speed controller (Pine Research Instrumentation Inc., Grove City, PA, USA). In RRDE measurement, Pt ring electrode was kept at +0.80 V for the oxidation of peroxide produced at the disk electrode. All experiments were carried out at room temperature.

3. Results and discussion

3.1. Surface morphology of RGSs

Fig. 1 shows height tapping-mode AFM image of synthesized RGSs deposited on mica. Nanosheets are flat and of uniform height relative to the mica substrate (~0.7–0.8 nm). In accordance with previous reports [38–40], these objects were interpreted to be single-layer sheets. The small particles in the sheets are caused by overexposure to sonication.

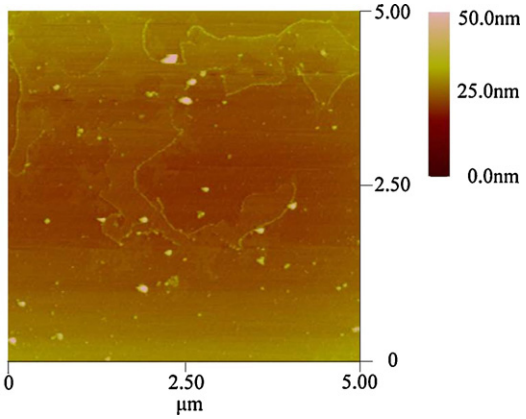

Fig. 1. AFM image of RGSs deposited on freshly cleaved mica.

3.2. Cyclic voltammetry for the ORR

Cyclic voltammograms obtained at bare GC and RGSs/GC electrodes in N_2-saturated and O_2-saturated 3.5% NaCl solutions are shown in Fig. 2. For the bare GC electrode, no reaction happens except that a small amount of hydrogen evolves at potentials more negative than −1.20 V in N_2-saturated solution (curve *a*). However, in O_2-saturated solution, there are three cathodic peaks at ca. −0.39, −0.71, and −1.40 V in the potential window employed (curve *b*). The first peak at −0.39 V can be attributed to a 2-electron electrochemical reduction of O_2 to H_2O_2, mediated by the active surface quinone-like groups with superoxide anion ($O_2\bullet^-$) as the intermediate (reaction (I, II)) [41]. At the second step, O_2 is transformed into H_2O_2 by a direct 2-electron reduction (reaction (III)) at the GC surface. Finally, H_2O_2 is reduced to H_2O at the third stage (reaction (IV)):

$$O_2 + e^- \rightarrow O_2\bullet^- \quad \text{(I)}$$

$$O_2\bullet^- + 2H^+ + e^- \rightarrow H_2O_2 \quad \text{(II)}$$

$$O_2 + 2H^+ + 2e^- \rightarrow H_2O_2 \quad \text{(III)}$$

$$H_2O_2 + 2H^+ + 2e^- \rightarrow 2H_2O \quad \text{(IV)}$$

Similar to the bare GC electrode, the RGSs/GC electrode presents no obvious cathodic peaks in N_2-saturated solution (curve *c*). At this electrode, the ORR also undergoes three steps. The first reduction process at −0.27 V is redox mediated by quinone-like groups at RGSs surface (reaction (I, II)), which is consistent with the previous report [32]. The second peak at −0.71 V and the third at −1.12 V cor-

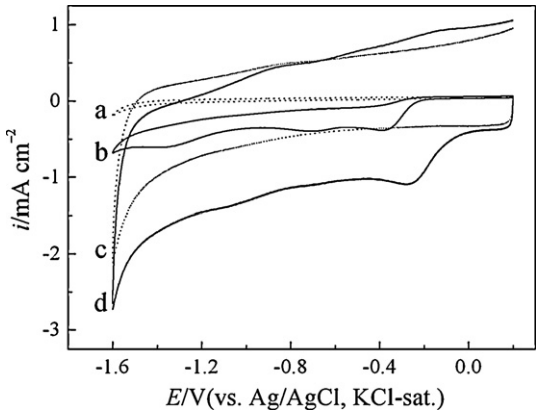

Fig. 2. Cyclic voltammograms recorded at bare GC (*a* and *b*) and RGSs/GC (*c* and *d*) electrodes in N_2- (*a* and *c*) and O_2-saturated (b and d) 3.5% NaCl solutions. Scan rate: 50 mV s^{-1}.

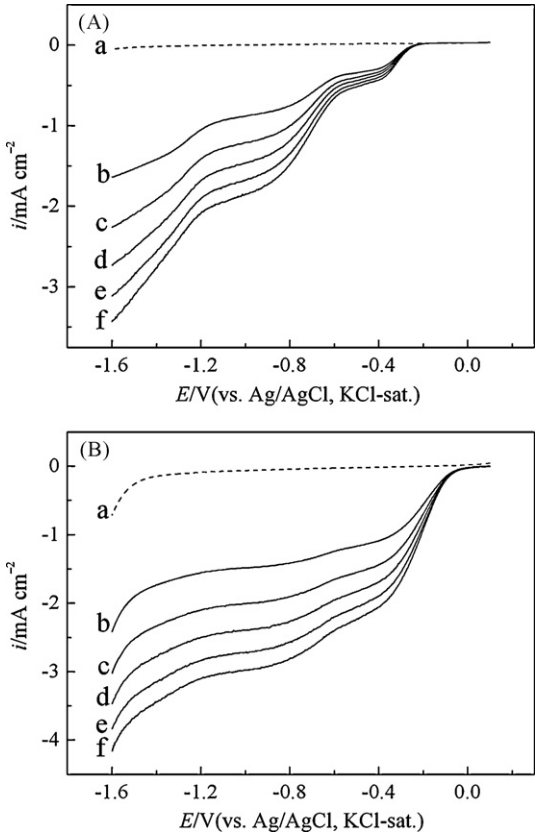

Fig. 3. RDE voltammograms at bare GC (A) and RGSs/GC disk electrodes (B) in N_2-(*a*) and O_2-saturated (*b–f*) 3.5% NaCl solutions at rotation rate of (*b*) 200 rpm, (*a*) and (*c*) 400 rpm, (*d*) 600 rpm, (*e*) 800 rpm, and (*f*) 1000 rpm. Scan rate: 10 mV s^{-1}.

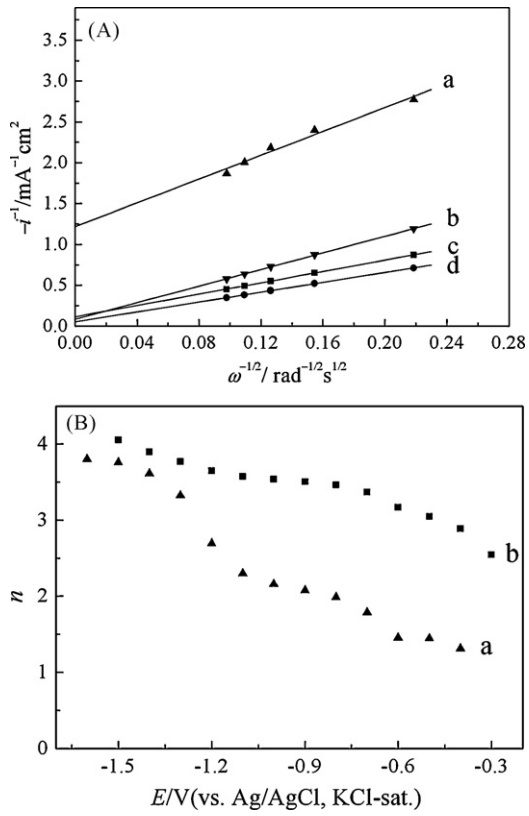

Fig. 4. (A) K–L plots for the ORR at different potentials (*a* and *c*, −0.50 V; *b* and *d*, −0.90 V) on bare GC (*a* and *b*) and RGSs/GC (*c* and *d*) electrodes. (B) Potential dependence of *n* on bare GC (*a*) and RGSs/GC (*b*) electrodes. Data obtained from Fig. 3.

respond to a direct 2-electron reduction of O_2 (reaction (III)) and the reduction of H_2O_2 to H_2O (reaction (IV)), respectively. By comparison, the modification of RGSs greatly increases the peak current and makes the peak potential shift by ca. 120 mV in the positive direction. These results suggest that RGSs have good catalytic activity towards the ORR.

3.3. RDE voltammetry and electron transfer number for the ORR

The mechanism of the ORR was further studied with RDE voltammetry and the results are shown in Fig. 3. Similar to the results obtained with cyclic voltammetry, three reduction steps are recorded at these two electrodes. This modification with RGSs results in an obvious positive shift of the half-wave potential and a larger current density. These differences may be attributed to quinone-like groups and a higher surface area of RGSs.

The Koutecky–Levich (K–L) plots for bare GC and RGSs/GC electrodes at −0.50 and −0.90 V are shown in Fig. 4A. The total number (*n*) of electrons transferred for the ORR can be estimated from the K–L equation:

$$\frac{1}{i} = \frac{1}{i_k} + \frac{1}{0.62nFC_0D_0^{2/3}\nu^{-1/6}\omega^{1/2}} \quad (1)$$

where *i* is the measured current density, i_k is the current density in the absence of any mass-transfer effects, ω is the angular velocity of rotation, and *F* is the Faraday constant (96485 C mol^{-1}). The values of the concentration of O_2 (C_0) and the diffusion coefficient of O_2 (D_0) in 3.5% NaCl solution are cited as 0.938×10^{-3} M and 2.17×10^{-5} cm^2 s^{-1} [42,43]. The value of the kinematic viscosity (ν) of 3.5% NaCl solution measured at our laboratory is 0.00956 cm^2 s^{-1}. The dependence of *n* on potential is shown in Fig. 4B.

The K–L plots for both the bare GC and the RGSs/GC electrode are almost linear, and the intercepts of the extrapolated lines at −0.90 V are close to zero, indicating the process is almost entirely under the control of mass-transfer. As shown in Fig. 4B, the variations of *n* with potential on these two electrodes are different. For the bare GC electrode, the plot can be divided into three stages. At potentials more positive than −0.60 V, between −0.80 and −1.00 V, and more negative than −1.40 V, the values of *n* are ca. 1.5, 2.0, and 4.0, respectively. These results are in good agreement with those from cyclic voltammetry. However, it is not that easy to identify three stages for the RGSs/GC electrode. The value of *n* can reach to 3.0 at −0.50 V, demonstrating a part of H_2O_2 produced can be transformed into H_2O via the catalysis of RGSs. Based on the analysis above, the reduction of H_2O_2 to H_2O occurs at the third stage, so we ascribe it to the disproportionation of the H_2O_2 (reaction (V)). At potentials between −0.80 and −1.10 V, the values of *n* are almost the same, which means the production and disproportionation of H_2O_2 are in equilibrium. At more negative potentials, the values of *n* have further increase due to the reduction of H_2O_2.

$$2H_2O_2 \rightarrow 2H_2O + O_2 \quad (V)$$

3.4. RRDE voltammetry for the ORR

The RRDE voltammograms for the ORR obtained at the bare GC disk electrode, the RGSs/GC disk electrode, and Pt ring electrodes in 3.5% NaCl solution are shown in Fig. 5. For both electrodes, ring current exhibits two oxidation peaks, demonstrating O_2 is reduced to H_2O_2 via two pathways. This result also suggests our definition of the first two peaks in cyclic voltammograms is reasonable. At potentials more negative than −1.20 V, the ring current decreases sharply, which again confirms that the reduction of H_2O_2 occurs

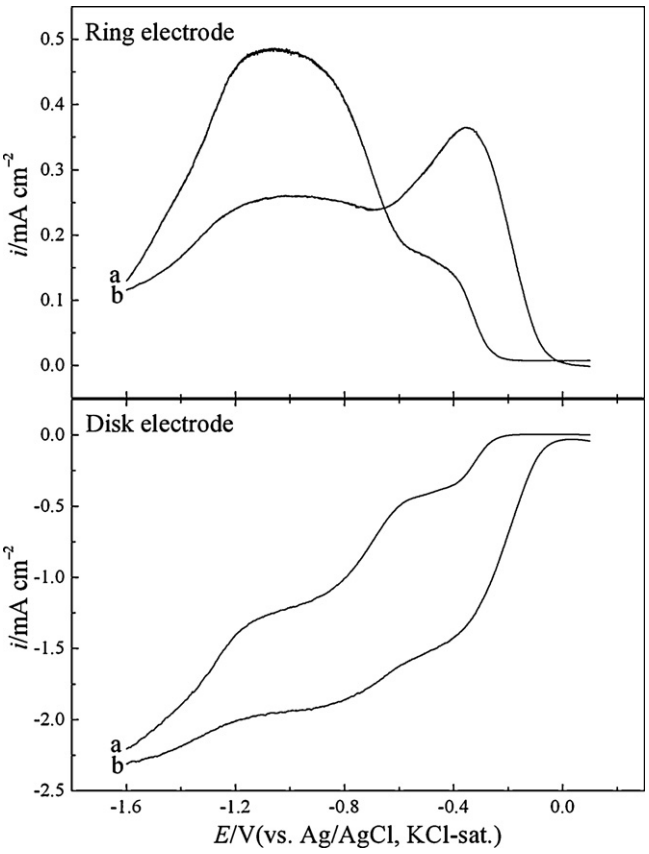

Fig. 5. RRDE voltammograms with a rotation rate of 400 rpm for the ORR at bare GC-Pt RRDE (*a*) and RGSs/GC-Pt RRDE (*b*) in O_2-saturated 3.5% NaCl solution. Scan rate: 10 mV s^{-1}.

at this step. By comparison, the modification of RGSs results in an obvious increase of the ring current at the first reduction step and a decrease at the second stage, which indicates that RGSs can effectively catalyze the formation of $O_2\bullet^-$ and the disproportionation of H_2O_2. These results showed that RGSs are a kind of bifunctional catalyst towards the ORR.

4. Conclusions

The present work demonstrates that RGSs have high catalytic activity towards the ORR in neutral media. RGSs were found to possess excellent catalytic activity for the disproportionation of H_2O_2, which facilitates the 4-electron ORR with a low overpotential. This work not only provides an insight into the mechanism of the ORR catalyzed by RGSs, but also offers theoretical basis for the future application of graphene as cathode materials for MFCs.

Acknowledgments

This work was supported by National Natural Science Foundation of China (No. 40876041) and National Key Technology R&D Program of China (No. 2007BAB27B01).

References

[1] C.E. Reimers, L.M. Tender, S. Fertig, W. Wang, Environ. Sci. Technol. 35 (2001) 192–195.
[2] H. Liu, R. Ramnarayanan, B.E. Logan, Environ. Sci. Technol. 38 (2004) 2281–2285.
[3] K. Rabaey, P. Clauwaert, P. Aelterman, W. Verstraete, Environ. Sci. Technol. 39 (2005) 8077–8082.
[4] B.E. Logan, J.M. Regan, Environ. Sci. Technol. 40 (2006) 5172–5180.
[5] G.C. Gil, I.S. Chang, B.H. Kim, M. Kim, J.K. Jang, H.S. Park, H.J. Kim, Biosens. Bioelectron. 18 (2003) 327–334.
[6] T.H. Pham, J.K. Jang, I.S. Chang, B.H. Kim, J. Microbiol. Biotechnol. 14 (2004) 324–329.
[7] J.C. Biffinger, J. Pietron, R. Ray, B. Little, B.R. Ringeisen, Biosens. Bioelectron. 22 (2007) 1672–1679.
[8] H. Rismani-Yazdi, S.M. Carver, A.D. Christy, I.H. Tuovinen, J. Power Sources 180 (2008) 683–694.
[9] F. Harnisch, S. Wirth, U. Schroder, Electrochem. Commun. 11 (2009) 2253–2256.
[10] E.H. Yu, S. Cheng, B.E. Logan, K. Scott, J. Appl. Electrochem. 39 (2009) 705–711.
[11] K.Y. Cheng, G. Ho, R. Cord-Ruwisch, Environ. Sci. Technol. 44 (2010) 518–525.
[12] Z. He, L.T. Angenent, Electroanalysis 18 (2006) 2009–2015.
[13] B. Erable, I. Vandecandelaere, M. Faimali, M.L. Delia, L. Etcheverry, P. Vandamme, A. Bergel, Bioelectrochemistry 78 (2010) 51–56.
[14] F. Zhao, F. Harnisch, U. Schroder, F. Scholz, P. Bogdanoff, I. Herrmann, Electrochem. Commun. 7 (2005) 1405–1410.
[15] E. HaoYu, S. Cheng, K. Scott, B. Logan, J. Power Sources 171 (2007) 275–281.
[16] K. Scott, I. Cotlarciuc, I. Head, K.P. Katuri, D. Hall, J.B. Lakeman, D. Browning, J. Chem. Technol. Biotechnol. 83 (2008) 1244–1254.
[17] F. Harnisch, N.A. Savastenko, F. Zhao, H. Steffen, V. Brusser, U. Schroder, J. Power Sources 193 (2009) 86–92.
[18] Y. Yuan, S.G. Zhou, L. Zhuang, J. Power Sources 195 (2010) 3490–3493.
[19] I. Roche, K. Scott, J. Appl. Electrochem. 39 (2009) 197–204.
[20] X. Li, B.X. Hu, S. Suib, Y. Lei, B.K. Li, J. Power Sources 195 (2010) 2586–2591.
[21] I. Roche, K. Katuri, K. Scott, J. Appl. Electrochem. 40 (2010) 13–21.
[22] J.M. Morris, S. Jin, J.Q. Wang, C.Z. Zhu, M.A. Urynowicz, Electrochem. Commun. 9 (2007) 1730–1734.
[23] S. Freguia, K. Rabaey, Z. Yuan, J. Keller, Electrochim. Acta 53 (2007) 598–603.
[24] B. Erable, N. Duteanu, S.M.S. Kumar, Y.J. Feng, M.M. Ghangrekar, K. Scott, Electrochem. Commun. 11 (2009) 1547–1549.
[25] K.S. Novoselov, A.K. Geim, S.V. Morozov, D. Jiang, Y. Zhang, S.V. Dubonos, I.V. Grigorieva, A.A. Firsov, Science 306 (2004) 666–669.
[26] A.K. Geim, K.S. Novoselov, Nat. Mater. 6 (2007) 183–191.
[27] J.F. Wang, S.L. Yang, D.Y. Guo, P. Yu, D. Li, J.S. Ye, L.Q. Mao, Electrochem. Commun. 11 (2009) 1892–1895.
[28] M.D. Stoller, S.J. Park, Y.W. Zhu, J.H. An, R.S. Ruoff, Nano Lett. 8 (2008) 3498–3502.
[29] Y. Wang, Y. Wan, D. Zhang, Electrochem. Commun. 12 (2010) 187–190.
[30] M.J. McAllister, J.L. Li, D.H. Adamson, H.C. Schniepp, A.A. Abdala, J. Liu, M. Herrera-Alonso, D.L. Milius, R. Car, R.K. Prud'homme, I.A. Aksay, Chem. Mater. 19 (2007) 4396–4404.
[31] R. Kou, Y.Y. Shao, D.H. Wang, M.H. Engelhard, J.H. Kwak, J. Wang, V.V. Viswanathan, C.M. Wang, Y.H. Lin, Y. Wang, I.A. Aksay, J. Liu, Electrochem. Commun. 11 (2009) 954–957.
[32] L.H. Tang, Y. Wang, Y.M. Li, H.B. Feng, J. Lu, J.H. Li, Adv. Funct. Mater. 19 (2009) 2782–2789.
[33] L.T. Qu, Y. Liu, J.B. Baek, L.M. Dai, ACS Nano 4 (2010) 1321–1326.
[34] Y.Y. Shao, S. Zhang, C.M. Wang, Z.M. Nie, J. Liu, Y. Wang, Y.H. Lin, J. Power Sources 195 (2010) 4600–4605.
[35] C.S. Shan, H.F. Yang, J.F. Song, D.X. Han, A. Ivaska, L. Niu, Anal. Chem. 81 (2009) 2378–2382.
[36] S. Stankovich, D.A. Dikin, R.D. Piner, K.A. Kohlhaas, A. Kleinhammes, Y. Jia, Y. Wu, S.T. Nguyen, R.S. Ruoff, Carbon 45 (2007) 1558–1565.
[37] W.S. Hummers, R.E. Offeman, J. Am. Chem. Soc. 80 (1958) 1339–11339.
[38] D. Li, M.B. Muller, S. Gilje, R.B. Kaner, G.G. Wallace, Nat. Nanotechnol. 3 (2008) 101–105.
[39] J.I. Paredes, S. Villar-Rodil, P. Solis-Fernandez, A. Martinez-Alonso, J.M.D. Tascon, Langmuir 25 (2009) 5957–5968.
[40] J.F. Shen, Y.Z. Hu, M. Shi, X. Lu, C. Qin, C. Li, M.X. Ye, Chem. Mater. 21 (2009) 3514–3520.
[41] F. Kuang, D. Zhang, Y.J. Li, Y. Wan, B.R. Hou, J. Solid State Electrochem. 13 (2009) 385–390.
[42] A.J. Vanstroe, L.J.J. Janssen, Anal. Chim. Acta 279 (1993) 213–219.
[43] S.L. Gojkovic, S.K. Zecevic, M.D. Obradovic, D.M. Drazic, Corros. Sci. 40 (1998) 849–860.